Developmental Biology 358 (2011) 331–343

Contents lists available at SciVerse ScienceDirect

Developmental Biology

journal homepage: www.elsevier.com/developmentalbiology

# The cytoplasmic domain of TGFβR3 through its interaction with the scaffolding protein, GIPC, directs epicardial cell behavior

Nora S. Sánchez [a], Cynthia R. Hill [a], Joseph D. Love [a], Jonathan H. Soslow [b], Evisabel Craig [c,d], Anita F. Austin [a,e], Christopher B. Brown [b], Andras Czirok [f,g], Todd D. Camenisch [c,d], Joey V. Barnett [a,*]

[a] Department of Pharmacology, Vanderbilt University Medical Center, Nashville, TN 37232, USA
[b] Department of Pediatrics, Vanderbilt University Medical Center, Nashville, TN 37232, USA
[c] Department of Pharmacology and Toxicology, University of Arizona, Tucson, AZ 85721, USA
[d] Steele Children's Research Center and Bio5 Institute, University of Arizona, Tucson, AZ 85721, USA
[e] Department of Cardiovascular Biology, Meharry Medical College, Nashville, TN 37208, USA
[f] Department of Anatomy and Cell Biology, University of Kansas Medical Center, Kansas City, KS 66160, USA
[g] Department of Biological Physics, Eotvos University, Budapest, Hungary

ARTICLE INFO

*Article history:*
Received for publication 14 May 2011
Revised 18 July 2011
Accepted 10 August 2011
Available online 25 August 2011

*Keywords:*
Coronary vessels
Epicardium
TGFβ
TGFβR3

ABSTRACT

The epicardium is a major contributor of the cells that are required for the formation of coronary vessels. Mice lacking both copies of the gene encoding the Type III Transforming Growth Factor β Receptor (TGFβR3) fail to form the coronary vasculature, but the molecular mechanism by which TGFβR3 signals coronary vessel formation is unknown. We used intact embryos and epicardial cells from E11.5 mouse embryos to reveal the mechanisms by which TGFβR3 signals and regulates epicardial cell behavior. Analysis of E13.5 embryos reveals a lower rate of epicardial cell proliferation and decreased epicardially derived cell invasion in *Tgfbr3*$^{-/-}$ hearts. *Tgfbr3*$^{-/-}$ epicardial cells *in vitro* show decreased proliferation and decreased invasion in response to TGFβ1 and TGFβ2. Unexpectedly, loss of TGFβR3 also decreases responsiveness to two other important regulators of epicardial cell behavior, FGF2 and HMW-HA. Restoring full length TGFβR3 in *Tgfbr3*$^{-/-}$ cells rescued deficits in invasion *in vitro* in response TGFβ1 and TGFβ2 as well as FGF2 and HMW-HA. Expression of TGFβR3 missing the 3 C-terminal amino acids that are required to interact with the scaffolding protein GIPC1 did not rescue any of the deficits. Overexpression of GIPC1 alone in *Tgfbr3*$^{-/-}$ cells did not rescue invasion whereas knockdown of GIPC1 in *Tgfbr3*$^{+/+}$ cells decreased invasion in response to TGFβ2, FGF2, and HMW-HA. We conclude that TGFβR3 interaction with GIPC1 is critical for regulating invasion and growth factor responsiveness in epicardial cells and that dysregulation of epicardial cell proliferation and invasion contributes to failed coronary vessel development in *Tgfbr3*$^{-/-}$ mice.



## Introduction

Coronary vessel development begins when a group of mesothelial cells known as the proepicardium are transferred to the surface of the heart where they form an epithelial sheet termed as the epicardium (Manner, 1993; Olivey et al., 2004; Tomanek, 2005; Viragh and Challice, 1981). A subset of these cells undergoes epithelial to mesenchymal transformation (EMT) and invades the subepicardial space with some of these cells continuing into the myocardium. Cells may differentiate into several cell lineages (Cai et al., 2008; Christoffels et al., 2009; Gittenberger-de Groot et al., 1998; Grieskamp et al., 2011; Lie-Venema et al., 2007, 2008) including vascular smooth muscle cells and cardiac fibroblasts (Mikawa and Fischman, 1992; Poelmann et al., 1993). The origin of endothelial cells is controversial (Lavine et al., 2008; Tomanek et al., 2006; Xiong, 2008), but recent work (Red-Horse et al., 2010) demonstrates that these cells arise from the sinus venosus. Together these cells contributed by the epicardium and sinus venosus are coordinately regulated to form the coronary vasculature.

Deletion of the gene encoding the Type III Transforming Growth Factor β Receptor (TGFβR3) in mice is embryonically lethal due to failed coronary vessel development (Compton et al., 2007). TGFβR3 contains a heavily glycosylated extracellular domain and a highly conserved, 43

*Abbreviations:* FGF, Fibroblast Growth Factor; FGFR, Fibroblast Growth Factor Receptor; GFP, Green Fluorescent Protein; GIPC, GTPase activated protein for Gαi subunits interacting protein C-terminus; HMW-HA, High Molecular Weight Hyaluronic Acid; IGF-IR, Insulin growth factor receptor, type I; PDGF, Platelet-Derived Growth Factor; PDGFR, Platelet-Derived Growth Factor Receptor; SM22α, Smooth Muscle 22 kDa actin-binding protein; SMαA, Smooth Muscle Alpha Actin; TGFBR1, Transforming Growth Factor-Beta Receptor I; TGFβR2, Transforming Growth Factor-Beta Receptor II; TGFβR3, Transforming Growth Factor-Beta Receptor III; TGFβ, Transforming Growth Factor-Beta; TUNEL, Terminal deoxynucleotidyl transferase-mediated dUridine Triphosphate Nick End Labeling; VEGF, Vascular Endothelial Growth Factor; WT-1, Wilm's Tumor-1; ZO-1, Zonula Occludins-1.

* Corresponding author at: Department of Pharmacology, Vanderbilt University Medical Center, Room 476 RRB, 2220 Pierce Avenue, Nashville, TN 37232-6600, USA. Fax: +1 615 343 6532.
*E-mail address:* joey.barnett@vanderbilt.edu (J.V. Barnett).

0012-1606/$ – see front matter © 2011 Elsevier Inc. All rights reserved.
doi:10.1016/j.ydbio.2011.08.008

amino acid intracellular domain with no known catalytic activity (Lopez-Casillas et al., 1991; Wang et al., 1991). TGFβR3 is required for the high affinity binding of TGFβ2 but also binds TGFβ1 and TGFβ3 (Lopez-Casillas et al., 1993). In addition, TGFβR3 can bind and signal in response to BMP2 (Kirkbride et al., 2008) and function as an inhibin receptor (Wiater et al., 2006). Upon binding TGFβ, TGFβR3 presents ligand to the Type I (TGFβR1) and Type II (TGFβR2) TGFβ Receptors to augment signaling via the canonical signaling pathway that is dependent on the phosphorylation and nuclear translocation of the Smads (Derynck and Zhang, 2003). Deletion of the cytoplasmic domain does not inhibit the ability of TGFβR3 to present ligand to TGFβR1 and TGFβR2 and subsequently augment the canonical signaling pathway (Blobe et al., 2001b). The results of targeting TGFβR3 in mice (Compton et al., 2007) and cardiac cushion explants (Brown et al., 1999) demonstrate a unique and non-redundant role for TGFβR3 in addition to ligand presentation. Regulation of the migration and invasion of several cancer cell lines has been shown to require the cytoplasmic domain of TGFβR3 (Lee et al., 2009a; Mythreye and Blobe, 2009) suggesting the presence of a noncanonical signaling pathway activated by TGFβR3.

Efforts to understand this noncanonical pathway downstream of TGFβR3 have focused on the identification of proteins that interact with the cytoplasmic domain of the receptor. Phosphorylation of Thr841 by TGFβR2 has been shown to be required for βarrestin2 binding and leads to TGFβR3 internalization and down-regulation of TGFβ signaling (Chen et al., 2003). The 3 C-terminal amino acids of TGFβR3, STA, serve as a Class I PDZ binding motif and bind the scaffolding protein, GIPC (GAIP-interacting protein, C terminus) (Blobe et al., 2001a). Interaction with GIPC stabilizes TGFβR3 at the surface and enhances TGFβ signaling (Blobe et al., 2001a). The interaction between TGFβR3 and either βarrestin2 (You et al., 2009) or GIPC (Lee et al., 2009a; Mythreye and Blobe, 2009) have been reported to regulate cell behavior, specifically proliferation, invasion and cell migration in breast and ovarian cancer cell lines.

Here we demonstrate that the loss of TGFβR3 results in decreased proliferation and invasion in intact embryos and cultured epicardial cells. The decreased invasion of epicardial cells *in vitro* is seen in response to not only TGFβ1 and TGFβ2 but also FGF2 and HMW-HA suggesting a dysregulation of key regulators of epicardial cell behavior following the loss of TGFβR3. The restoration of the invasive response to all these ligands in *Tgfbr3*$^{-/-}$ cells was shown to be dependent on the cytoplasmic domain of TGFβR3, specifically the 3 terminal amino acids, and interaction with GIPC. Based on our observations we propose that failed coronary vessel development in *Tgfbr3*$^{-/-}$ mice is at least partly due to decreased epicardial cell proliferation and mesenchymal cell invasion which provides fewer cells to participate in coronary vessel development.

## Materials and methods

### *Generation of embryos*

*Tgfbr3*$^{+/-}$ mice were generated as described (Compton et al., 2007) and maintained on a C57BL/6 SV129 mixed background. *Tgfbr3*$^{+/-}$ littermates were crossed to generate *Tgfbr3*$^{+/+}$ and *Tgfbr3*$^{-/-}$ embryos.

### *Cell culture*

Immortalized epicardial cell lines were obtained as previously described (Austin et al., 2008). To maintain the immortalized state, cells were grown in immorto media: DMEM containing 10% FBS (fetal bovine serum), 100 U/ml Penicillin/Streptomycin (P/S), 1× Insulin–Transferrin–Selenium (ITS; 1 μg/ml insulin, $5.5\times10-4$ μg/ml transferrin, 0.677 μg/ml selenium), and 10 U/ml (interferon γ) INFγ at 33 °C. For experiments, the T antigen was silenced by culturing at 37 °C in the absence of ITS or I INFγ. Multiple *Tgfbr3*$^{+/+}$ and *Tgfbr3*$^{-/-}$ littermate pairs were used where available. E11.5 epicardial cells were used in all experiments unless otherwise specified.

### *Growth factors*

TGFβ1, TGFβ2, and high molecular weight hyaluronic acid (HMW-HA) (~980 kDa) were purchased from R&D Systems. FGF-2, PDGF-AA, PDGF-BB, EGF, and VEGF were purchased from (Pepprotech).

### *Immunohistochemistry*

*Tgfbr3*$^{+/+}$ and *Tgfbr3*$^{-/-}$ cells were plated at a density of 25,000 cells per well in one well of a 4-well collagen coated chamber slide and allowed to adhere overnight at 37 °C. The following day the media was replaced with DMEM containing 5% FBS and incubated with vehicle (4 mM HCl/0.01% BSA), 250 pM TGFβ1 or TGFβ2. After a 72 hour incubation period at 37 °C, cells were fixed. For ZO-1 staining, cells were fixed in 70% methanol on ice for 10 min; for SM22α, 2% paraformaldehyde (PFA) for 30 min and permeabilized with PBS and 0.2% Triton X-100 for 5 min at room temperature. Cells immunostained for ZO-1 were blocked with 2% bovine serum albumin (BSA) in PBS for 1 h and incubated with dilute primary antibody (ZO-1, 2 μg/ml, Zymed) overnight at 4 °C. For SM22α (Abcam) cells were blocked with 5% horse serum, and incubated with primary antibody (SM22α, 1:200) overnight at 4 °C. Primary antibody detection was with goat anti-rabbit cy3 (ZO-1) or donkey anti-goat cy3 (SM22α) secondary antibody (1:800; Jackson ImmunoResearch). Cells infected with adenovirus co-expressing GFP and TGFβR3 were fixed in 2%PFA and stained for TGFβR3 (5 μg/ml, AF-242-PB, R&D) for 1 h at RT, and detected with Alexa555 conjugated donkey anti-goat antibody (Invitrogen) for 1 h at RT. Nuclei were stained with 4′,6-diamidino-2-phenylinodole (DAPI; Sigma). Photomicrographs were captured with Nikon Eclipse TE2000-E microscope and QED imagining software.

### *qRT-PCR*

*Tgfbr3*$^{+/+}$ and *Tgfbr3*$^{-/-}$ cells were seeded at 200,000 cells per well of a 6 well tissue culture plate and allowed to adhere overnight at 37 °C. The following day the media was replaced with DMEM containing 5% FBS and incubated with vehicle, 250 pM TGFβ1 or TGFβ2. After a 72 hour incubation period at 37 °C, total RNA was isolated using the TRIzol reagent (Invitrogen) according to the manufacturer's protocol. cDNA was generated from 1 μg total RNA using oligo-dT primers and Superscript III polymerase (Invitrogen). Real-time PCR analysis was done with iQ SYBR Green Supermix (Bio-Rad) in the Bio-Rad iCycler for 40 cycles. The expression levels are calculated using the $\Delta\Delta C_T$ method. The threshold cycle ($C_T$) represents the PCR cycle at which an increase of the reporter fluorescence above the baseline is first detected. The fold change in expression levels, R, is calculated as follows: $R=2^{-\Delta\Delta CT}$ (where $R=2^{(\Delta CT\ \text{treated}\ -\ \Delta CT\ \text{control})}$). This method normalizes the abundance of all transcripts to the constitutive expression level of *GAPDH* RNA. Primer pairs for the smooth muscle markers, Sm22α, SMαA, and calponin are as follows:

| Gene | Sense primer (5′→3′) | Anti-sense primer (5′→3′) |
|---|---|---|
| *Sm-22α* | AGCCAGTGAAGGTGCCTGAGAAC | TGCCCAAAGCCATTAGAGTCCTC |
| *SmαA* | GAGAAGCCCAGCCAGTCG | CTCTTGCTCTGGGCTTCA |
| *Calponin* | GAAGGCAGGAACATCATTGGACTG | CTCAAAGATCTGCCGCTTGGTGCC |
| *GAPDH* | ATGACAATGAATACGGCTACAG | TCTCTTGCTCAGTGTCCTTG |

### *Wound healing assay*

Cells were seeded in a 35-mm culture plate coated with collagen at a density of $3\times10^6$ cells/plate in immorto media and incubated at 33 °C.

Cells were allowed to form a confluent monolayer within 2 days. Upon reaching confluency, cells were starved with DMEM containing 0.5% FBS and 100 U/ml P/S and incubated overnight at 37 °C. Eight 1-mm circular cell free areas were created with a stabilized rotating silicone tip, and immediately photographed. Wound closure was monitored by for 72 h. The denuded area was measured using ImageJ software. Percent wound closure relative to the initial wound area was calculated. Experiments were repeated three times.

*Time lapse, two dimensional motility assay*

Cells were seeded in 35 mm culture plates, either coated with collagen or containing 1 ml collagen gel, prepared at a density of 1.75 mg/ml as described (Runyan and Markwald, 1983). Two or four sister cultures, containing cells derived from littermate embryos, were recorded with an automated inverted microscope system (Leica DMIRE2, Leica Microsystems, Germany) equipped with a stage-attached incubator (Perryn et al., 2008). Images (608×512 pixels spatial and 12 bit intensity resolution) were obtained with a 10× objective (0.30 N.A.) and a cooled Retiga 1300 camera (QImaging, Burnaby, British Columbia). The control software recorded multiple microscopic fields within each culture dish. The time lag between consecutive image frames was 10 min.

Cell movements were obtained from the recorded image sequences by two independent procedures. Manual cell tracking (Perryn et al., 2008) results in cell trajectories over long time periods, but the number of cells tracked is limited to 20–30 per field, around 10% of the cells present. An automated flow field estimator (Particle Image Velocimetry (PIV) algorithm (Zamir et al., 2005), combined with a cell/background segmenter (Wu et al., 1995) yields unbiased velocity fields over the entire cell covered area, without distinguishing individual cells.

Cell displacements can be characterized by the mean magnitudes of displacements during various time intervals as $d(\tau)=\{|x_i(t+\tau)-x_i(t)|\}_{i,t}$ where $x_i(t)$ denotes the position of cell $i$ at various time points $t$, and the average $\{\}_{i,t}$ is calculated for all possible choices of $i$ and $t$ (Rupp et al., 2008). Speed values are defined as $d(\tau=1\,\mathrm{h})$, *i.e.*, mean cell displacements during a 1 hour long time period (6 frames). The PIV method directly yields speed values (albeit not for each cell but rather per unit area) when the compared images were recorded 1 h apart.

For statistical purposes, we compared mean speed values obtained from independent time lapse recordings ($n\geq 3$).

*Proliferation*

*BrdU incorporation in vitro*

Cells were plated in 4-well collagen coated chamber slides at a density of 25,000 cells/well and were allowed to attach overnight at 37 °C in DMEM containing 10% FBS and 100 U/ml Penn/Strep. To synchronize at $G_0$, 24 h post-plating, cells were serum starved in DMEM containing 0.5% FBS and 100 U/ml Penn/Strep overnight, followed by replacement of DMEM containing 10% FBS and 100 U/ml P/S. Cells were fixed in ethanol at 24, 48 and 72 h after replacing growth medium. BrdU (bromodeoxyuridine) incorporation assay was carried out as instructed by manufacturer (Roche: BRDU Labeling and Detection Kit II). Random fields were selected and photographed for each well using Nikon Eclipse TE2000-E microscope and QED imaging software. Percent proliferation was calculated by counting the number of BrdU positive cells in a total of 500 cells per genotype at each time point. Experiments were repeated three times on cells from one littermate pair.

*MTS assay*

This method relies on the *in vivo* reduction of MTS tetrazolium to a colored formazan product by NADPH in metabolically active cells. The product formed is read at 490 nm and is directly proportional to the number of living cells in culture. Cells were plated in triplicate in a 96-well plate at a density of 5000 cells/well in 100 µl of DMEM containing 10% FBS and 100 U/ml P/S overnight at 37 °C. At 24, 48, and 72 h post-plating, 20 µl of substrate (Promega: Cell Titer 96 Aqueous Solution) was added to each well. Colorimetric reaction was allowed to proceed for 30 min at 37 °C, followed by reading at 490 nm. Experiments were repeated three times in triplicate per littermate pair. At least 3 different littermate pairs were analyzed.

*BrdU incorporation in vivo*

Pregnant mice at E12.5 and E13.5 were injected with BrdU 100 µg/kg at 6 h, 4 h, and 2 h before sacrifice. The embryos were genotyped and embedded and *Tgfbr3*$^{+/+}$ and *Tgfbr3*$^{-/-}$ littermate embryos were sectioned. Sections (7 µm) through the heart were blocked with 5% Normal Donkey Serum/1% BSA and immunostained with a rat Anti-BrdU antibody (Accurate Chemical & Scientific Corp; 1:200) and an AlexaFluor 594 Donkey Anti-Rat secondary antibody (Invitrogen, 1:200). DAPI was used to stain nuclei. Photographs of each section were acquired using Nikon Eclipse TE2000-E microscope at 20× magnification and QED imaging software. The total number of nuclei and the number of BrdU positive nuclei were determined in representative sections of the epicardium using Image J software. The percentage of BrdU positive nuclei were calculated as a measure of cell proliferation. Three animals per genotype, per stage were analyzed.

*Apoptosis assays*

*Caspase 3/7 homogenous assay*

Cells were plated in triplicate in a 96-well plate at a density of 10,000 cells/well in 100 µl of DMEM containing 10% FBS and 100 U/ml P/S overnight at 37 °C. At each time point, 24, 48, and 72 h post-plating, 100 µl of substrate (ApoONE Homogenous Caspase 3/7 Assay; Promega) was added to each well. Colorimetric reaction was allowed to proceed for 2 h at room temperature. Caspase 3/7 activity was then detected by reading the fluorescence of each well (Ex: 499 nm, Em: 521 nm). Experiments were repeated three times in triplicate per littermate pair. At least 3 different littermate pairs were analyzed.

*Trypan blue exclusion*

Cells were plated in duplicate in 12-well collagen coated plates a density of 100,000 cells/well and were allowed to attach overnight at 37 °C in DMEM containing 10% FBS and 100 U/ml Penn/Strep. At 24, 48 and 72 h post-plating, cell were trypsinized and re-suspended in 500 µl media. Trypan blue was added to cells at a 1:1 ratio and allowed to sit at room temperature for 1 min. Five hundred cells per genotype were counted at each time point, and the proportion of trypan blue positive cells to total cells was calculated Experiments were repeated three times in triplicate per littermate pair.

*TUNEL in vivo*

E12.5 and E13.5 embryos were genotyped, embedded, and *Tgfbr3*$^{+/+}$ and *Tgfbr3*$^{-/-}$ littermate embryos were sectioned. TUNEL staining was performed using DeadEnd Fluoremetric TUNEL System (Promega) on 7 µm sections through the heart and the nuclei stained with DAPI. Photographs of each section were acquired using Nikon Eclipse TE2000-E microscope and QED imaging software. The total number of nuclei and the number of TUNEL positive nuclei were determined in representative sections of the epicardium to determine the percentage of apoptotic cells present. Three animals per genotype, per stage were analyzed.

*Invasion assays*

*Calcein labeled/plate reader*

To determine the invasive potential of immortalized epicardial cells in response to growth factor stimulation, a modified Boyden

chamber assay was employed. Collagen gels were prepared as described (Craig et al., 2010b). Briefly, cells were fluorescently labeled with CalceinAM (BD Biosciences) and then plated at 12,000 cells per well in DMEM containing 0.5% FBS (fetal bovine serum) in the top chamber. Cells were then allowed to settle overnight at 37 °C. The following day, DMEM containing 20% FBS ± vehicle (4 mM HCl/0.1% BSA), 250 pM TGFβ1 or TGFβ2 (R&D Systems) or 10 ng/ml FGF-2, PDGF-AA, PDGF-BB, EGF, or VEGF was added to the bottom chamber and incubated for an additional 24 h at 37 °C. Cells receiving HMW-HA treatment were pre-treated with 300 μg/ml HMW-HA (unless otherwise specified) in DMEM containing 0.5% FBS in the top well for 30 min. Media was then removed and replaced with fresh DMEM containing 0.5% FBS. 300 μg/ml HMW-HA was then added to the bottom chamber as described for the other ligands. The top insert was then removed and placed in a plate containing 0.25% Trypsin/2.21 mM-EDTA in HBSS (CellGro). Cells were allowed to detach from the membrane into the trypsin containing plate, which was then read using SpectraMax 96-well plate reader (Ex: 485, Em: 538, Cutoff: 530; sensitivity: 30). Relative invasion was calculated by normalizing treatment to vehicle treated groups.

*Crystal violet stain*

Cells were plated as described above. Instead of placing wells in trypsin, membranes were fixed in 2.5% Gluteraldehyde (Sigma) for 2 min, rinsed once with 1× PBS then stained in 0.4% Crystal violet (Fisher) for 5 min, and mounted. Photographs of each membrane were acquired using Nikon Eclipse TE2000-E microscope and QED imaging software.

*WT-1 staining in vivo*

E13.5 embryos were genotyped, embedded, and *Tgfbr3*$^{+/+}$ and *Tgfbr3*$^{-/-}$ littermate embryos were sectioned. Sections through the heart were immunostained with a rabbit anti-WT-1 (Santa Cruz, 1:200) and the nuclei stained with DAPI. Photographs of each section were acquired using Nikon Eclipse TE2000-E microscope at 40× magnification and QED imaging software. The total numbers of WT-1 positive cells were determined in representative sections of the heart to determine the percentage of WT-1 positive cells invading the subepicardial space and myocardium.

*Expression analysis*

Expression levels of LYVE1, CD44, FGFR1, FGFR2b, FGFR2c, FGFR3 and FGFR4 were analyzed using qRT-PCR as described above. Primer sequences were previously published and purchased from IDT (Craig et al., 2010b; Quarto and Longaker, 2008).

| Gene | Sense primer (5′→3′) | Anti-sense primer (5′→3′) |
|---|---|---|
| *Lyve1* | *CAGCATTCAAGAACGAAGCAG* | *GCCTTCACATACCTTTTCACG* |
| *CD44* | *TCCTTCTTTATCCGGAGCAC* | *AGCTGCTGCTTCTGCTGTACT* |
| *Fgfr1* | *GTGGCCGTGAAGATGTTGAAGTCC* | *GCCGGCCGTTGGTGGTTTT* |
| *Fgfr2b* | *CACCCGGGGATAAATAGCTCCAATG* | *GCTGTTTGGGCAGGACAGT* |
| *Fgfr2c* | *CACCCCGGTGTTAACACCACGG* | *CTGGCAGAACTGTCAACCATG* |
| *Fgfr3* | *TGCCGGCCAACCAGACAGC* | *GCGCAGGCGGCAGAGTATCAC* |
| *Fgfr 4* | *ATGAGCCGGGGAGCAGCAATGTT* | *GGGGGATGGCAGGGGGTGGTG* |

*Western blots*

*Tgfbr3*$^{+/+}$ and *Tgfbr3*$^{-/-}$ littermate epicardial cells were lysed and diluted in TNEN buffer (1 M Tris base, 5 M NaCl, 0.5 M EDTA and NP40) as described (Craig et al., 2010b). Total cellular lysates were then resolved by sodium dodecyl sulfate-polyacrylamide gel electrophoresis (SDS-PAGE) and transferred onto a polyvinylidene difluoride (PVDF) membrane. After blocking in 3% BSA, membranes were probed with Rat anti-CD44 antibody (clone KM201) (Southern Biotech), rabbit anti-LYVE1 (XLKD1) Antibody (C-term) (Abgen). β-actin (Affinity Bio Reagents) was used as a loading control. TGFβR3 expression was confirmed using goat-polyclonal antibody (AF-242-PB) (R&D) and donkey anti-goat-HRP secondary R&D). Detection was performed using Super Signal West Pico substrate (Pierce).

*Adenovirus infections*

Adenoviruses were generated using the pAdEasy system (He et al., 1998). All concentrated viruses were tittered by performing serial dilutions of the concentrated virus and counting the number of GFP-expressing 293 cells after 18–24 h. The following adenoviruses co-expressing GFP were used: full length TGFβR3 (FL), TGFβR3 missing the cytoplasmic domain (CYTO) or the last 3 amino acids (Δ3), or GIPC. Cells were plated in collagen coated 6 well dishes at a density of 200,000 cells per well in immorto media overnight at 33 °C. The following day, virus was added directly to the cells at a final concentration of $10^8$ PFU/ml and allowed to incubate for an additional 24 h. The next day cells were plated for invasion or proliferation assays as described above.

*Transfections*

*siRNA*

Cells were plated at a density of 200,000 per well of 6-well plate. The following day cells were transfected with 2 μg siRNA (Ambion) and 8 μl Xtreme siRNA Transfection Reagent (Roche). Sequences for siRNA used are as follows: GIPC1: *sense* 5′-GCAGUGUGAUUGACCACAUtt-3′, *anti-sense* 5′-AUGUGGUCAAUCACACUGCct-3′. At 48 h post-transfection cells were harvested for qRT-PCR to confirm knockdown of Gipc1(sense, 5′-TGGTTCAGGCCCACAA-3′; anti-sense, 5′-TCTCTAGCAAGTCATCCACC-3′), or used directly for invasion assays. Where overexpression of TGFβR3 was done in conjunction with knockdown of GIPC1, cells were transfected with siRNA, then infected with adenovirus 24 h after, and plated for invasion assays 24 h after that.

*Plasmids*

Cells were plated at a density of 50,000 per well of 6-well plate. The following day cells were transfected with 2 μg pcDNA3.1 vector alone or expressing full length TGFβR3-F), TGFβR3-CYTO or TGFβR3-Δ3 and 8 μl FugeneHD Transfection Reagent (Roche). After 48 h, cells were harvested for Western blot analysis.

*Statistical analysis*

Paired student *t*-test was used to establish significance. Data are presented as the average of three experiments ± SEM for one littermate pair, unless otherwise specified. P-values of $<0.05$ were considered significant.

## Results

*Epicardial cells in Tgfbr3*$^{-/-}$ *embryos display decreased proliferation and invasion*

Deletion of *Tgfbr3* in the mouse results in death at E14.5 due to failed coronary vessel development that is characterized by an abnormal epicardium, increased subepicardial space, and poorly developed, dysmorphic vessels (Compton et al., 2007). These observations suggest that although the epicardium is formed in *Tgfbr3*$^{-/-}$ embryos, aberrant epicardial cell behavior may underlie the failure of coronary vessel development. Therefore we chose to measure epicardial cell proliferation, apoptosis, and invasion *in vivo* as an initial attempt to determine the mechanisms responsible for failed coronary vessel development. To determine the rate of epicardial cell proliferation, pregnant *Tgfbr3*$^{+/-}$ mice were injected with BrdU and embryos harvested at E12.5 and E13.5, a time when the epicardium covers the heart and epicardial cell

EMT is evident. Embryos were sectioned and immunostained for BrdU (Fig. 1A). Epicardial cells were counted and the percent of BrdU positive cells determined. No difference was noted at E12.5, however at E13.5 epicardial cells in *Tgfbr3*$^{+/+}$ embryos showed significantly more proliferation than *Tgfbr3*$^{-/-}$ littermates (25.3%±0.88% *vs* 15.7%±1.58%, p=0.012; n=3) (Fig. 1B). Apoptosis was assessed in E12.5 and E13.5 littermate embryos by TUNEL analysis. We noted a very low rate of apoptosis in *Tgfbr3*$^{+/+}$ embryos (<4%) and no significant difference between genotypes (Supplementary Fig. 1A). After the epicardium covers the surface of the heart *in vivo*, a subset of epicardial cells undergo EMT and invade the subepicardial space with some cells continuing into the myocardium (Olivey et al., 2004). We assessed epicardial cell invasion in E13.5 embryos by detecting the epicardial cell marker WT1 (Moore et al., 1999). *Tgfbr3*$^{-/-}$ embryos display a significantly lower number of WT-1 positive cells that invade the subepicardial space or the myocardium (20.4%±3.71) compared to *Tgfbr3*$^{+/+}$ littermates (31.0%±2.87) (Figs. 1C and D; Supplementary Figs. 2A and B). These data suggest that both decreased cell proliferation and decreased cell invasion contribute to failed coronary vessel development in *Tgfbr3*$^{-/-}$ mice.

### *Tgfbr3*$^{-/-}$ epicardial cells display decreased proliferation and invasion *in vitro*

Given the alterations in epicardial cell proliferation and invasion noted in *Tgfbr3*$^{-/-}$ embryos, we developed immortalized epicardial cell lines from *Tgfbr3*$^{+/+}$ and *Tgfbr3*$^{-/-}$ embryos that would allow us to probe TGFβR3 regulation of epicardial cell behavior *in vitro*. Since we have previously immortalized epicardial cells from *Tgfbr3*$^{+/+}$ embryos and shown that these cells behave similarly to freshly isolated primary cells (Austin et al., 2008), we used this same approach to generate and characterize epicardial cells from *Tgfbr3*$^{+/+}$ and *Tgfbr3*$^{-/-}$ littermate pair embryos. We first measured the proliferation rates of *Tgfbr3*$^{+/+}$ and *Tgfbr3*$^{-/-}$ epicardial cells. As measured by BrdU incorporation, *Tgfbr3*$^{+/+}$ cells exhibit proliferation rates that peak at 48 h and decline to basal levels by 72 h. *Tgfbr3*$^{-/-}$ cells show a significantly reduced rate of proliferation that is sustained throughout the time course examined (Figs. 2A and B). We used an MTS assay as a second independent approach to confirm this initial observation. *Tgfbr3*$^{-/-}$ cells had a cell density 50% lower at 48 h and 62% lower at 72 h, indicating an overall lower rate of

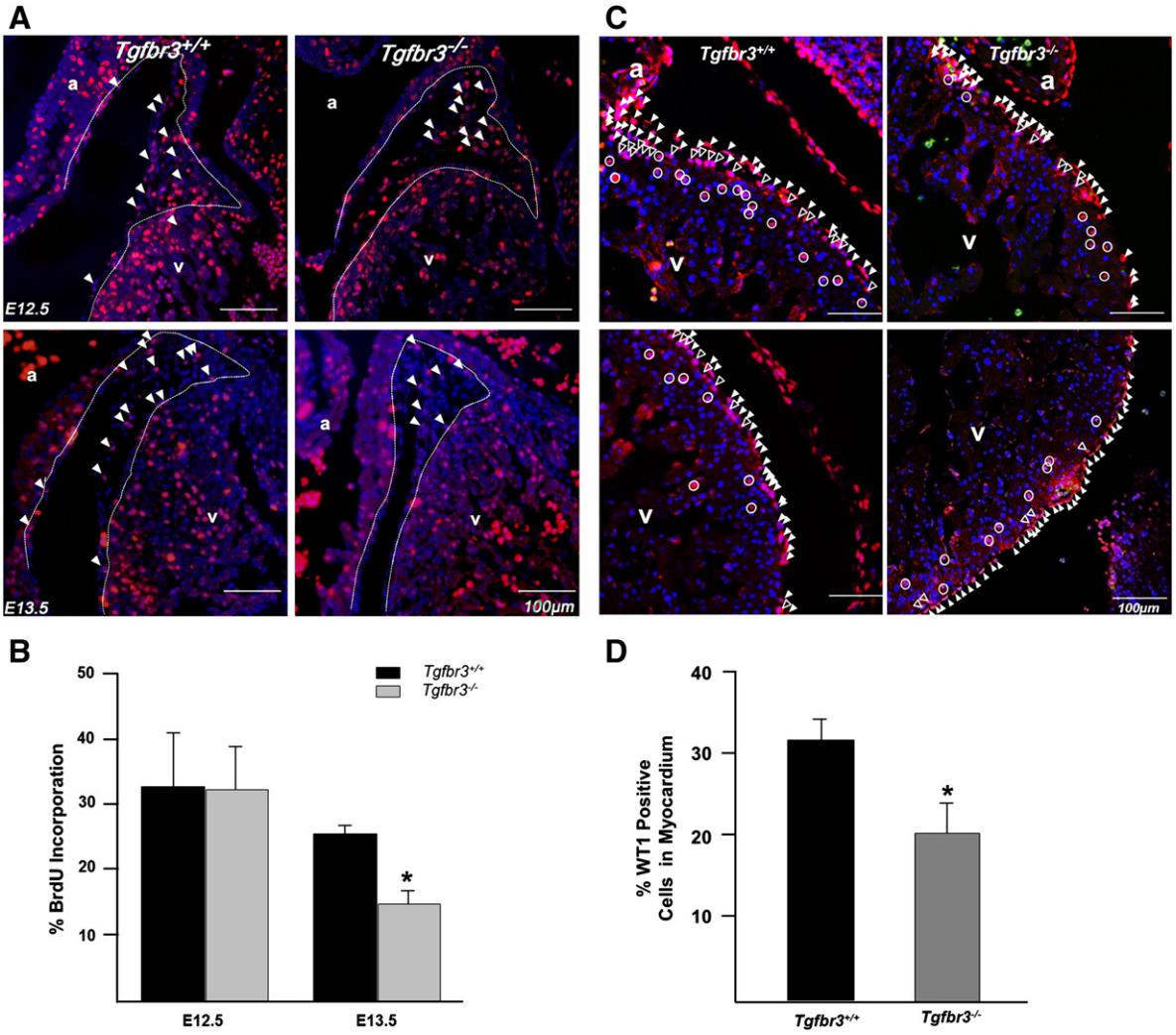


**Fig. 1.** Epicardial cells in *Tgfbr3*$^{-/-}$ embryos show decreased proliferation and invasion *in vivo*. (A) Heart sections from E12.5 and E13.5 embryos stained for BrdU. Representative BrdU positive cells are indicated by solid arrowheads. White dashed line demarcates myocardium from the epicardium and subepicardial space. (B) Percent proliferation is the number of BrdU positive cells per total number of DAPI stained nuclei (n=3 embryos per genotype, per stage (*p<0.05)). (C) Sections stained for WT1 in E13.5 hearts. Representative WT1 positive mesenchymal cells are identified by the open circles. Representative cells in the epicardium are indicated by solid arrowheads, while epicardially derived mesenchymal cells in the subepicardial space are identified by the open arrowheads. (D) Percent invasion into myocardium is calculated as the number of WT1 positive mesenchymal cells per total WT1 positive cells (n=3 embryos per genotype (*p<0.05)). (a = atria, v = ventricle).

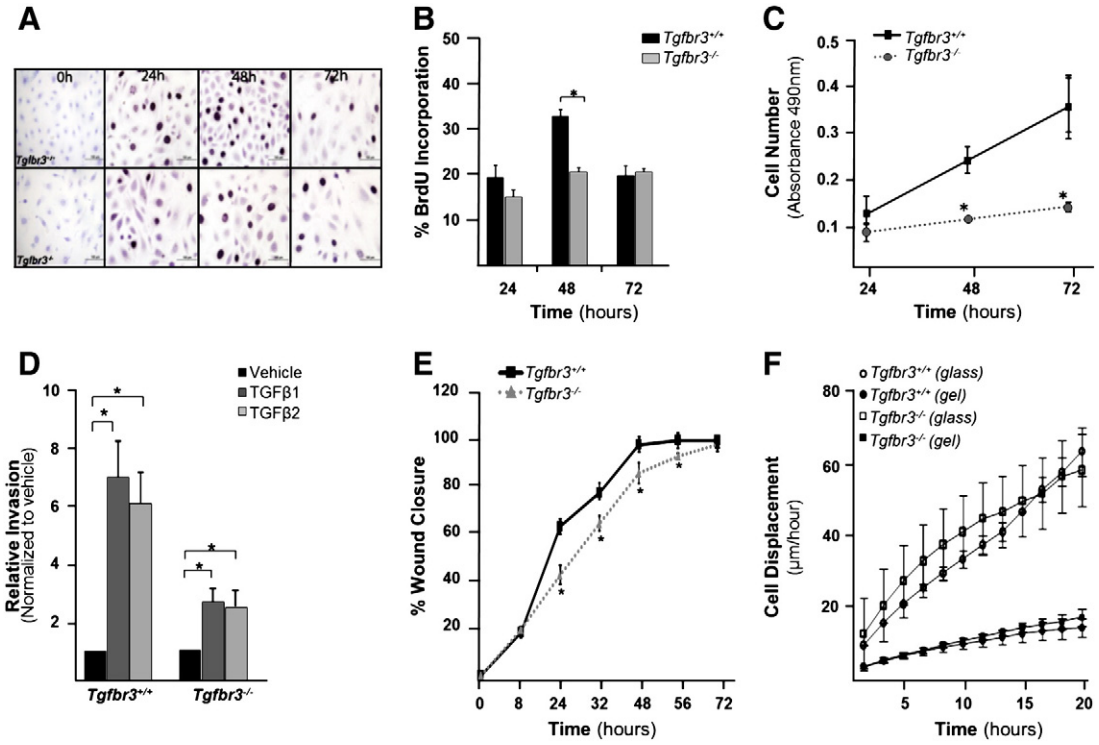


**Fig. 2.** Cultured *Tgfbr3*$^{-/-}$ epicardial cells show decreased proliferation and invasion. (A) Photomicrographs of cells incubated with BrdU and fixed at 24, 48 and 72 h after initial seeding on 4-well collagen coated slides. (B) Quantitation of percent BrdU incorporation (n = 3, *p = 0.001) (C) Measurement of cell number by MTS assay (experiments were repeated 3 times in triplicate, results for one littermate pair shown, *p<0.05). (D) Quantitation of invasion using a modified Boyden chamber assay of one littermate pair (experiments were repeated 3 times in replicates of 6, * = p<0.05). (E) Graph quantifying percent wound closure over 72 h after confluent cell monolayers were wounded using a rotating silicon tip (experiments were repeated three times, results for one littermate pair shown, *p<0.05). (F) Mean cell displacements values using live video microscopy of one littermate pair. The difference between genotypes is not significant.

proliferation throughout the time course of the experiment (Fig. 2C). We measured apoptosis *in vitro* through Caspase 3/7 activity and trypan blue exclusion (Supplementary Figs. 1B and C). *Tgfbr3*$^{-/-}$ cells have an elevated level of apoptosis at all-time points as measured by both methods. This increase in apoptosis was not seen *in vivo*. This may be partially explained by the inherent low levels of apoptosis that would make detecting small changes in apoptosis difficult. Alternatively, *in vitro* cells may respond to the stress inherent in culture by increasing apoptosis while cells *in vivo*, absent this stress, may have unaltered rates of apoptosis. To examine epicardial cell invasion we used a modified Boyden Chamber assay as a model system. Incubation of *Tgfbr3*$^{+/+}$ cells with either 250 pM TGFβ1 or TGFβ2 induces a 7 and 6 fold increase in cell invasion over vehicle, respectively. In contrast, epicardial cells from *Tgfbr3*$^{-/-}$ littermates incubated with either TGFβ1 or TGFβ2 induced only a 2-fold increase in invasion (Fig. 2D, Supplementary Fig. 3). The decreased proliferation and invasion seen in *Tgfbr3*$^{-/-}$ epicardial cells *in vitro* support the use of these cells as a model system to elucidate the mechanisms by which the loss of TGFβR3 alters proliferation and invasion *in vivo*.

Since *Tgfbr3*$^{-/-}$ epicardial cells show decreased invasion *in vitro* and *in vivo*, we asked whether *Tgfbr3*$^{-/-}$ cells displayed impaired motility in a 2 dimensional assay that does not require matrix invasion. We used an *in vitro* wound healing assay to initially probe epicardial cell motility. *Tgfbr3*$^{+/+}$ cells close a wound by 48 h. However cells from *Tgfbr3*$^{-/-}$ littermates require an additional 24 h (Fig. 2E and Supplementary Fig. 4A). Since wound closure may be affected by both cell motility and cell proliferation, we used time lapse video microscopy to determine the role of motility directly in the delay of wound healing. Four littermate cell line pairs were compared, and for each pair multiple independent time lapse recordings were used to compute average motility. In these 2-dimensional motility assays, *Tgfbr3*$^{-/-}$ cells from one littermate pair display a slightly faster motility rate (13%; p<0.001) (Supplementary Fig. 4B). The motility of *Tgfbr3*$^{+/+}$ and *Tgfbr3*$^{-/-}$ cells substantially increases on hard substrates: cells move on collagen coated glass threefold faster than on the surface of a collagen gel (Fig. 2F). However, in each case altered cell motility could not explain the delayed wound healing in *Tgfbr3*$^{-/-}$ cells, thus decreased wound healing is likely due to decreased rates of proliferation.

### *Tgfbr3*$^{-/-}$ *epicardial cells can undergo EMT and smooth muscle differentiation in response to TGFβ1 or TGFβ2*

Epicardial cells give rise to the vascular smooth muscle cells that are required for vessel stabilization and maintenance (Mikawa and Gourdie, 1996). Analysis of *Tgfbr3*$^{-/-}$ embryos suggest that epicardial cells do give rise to smooth muscle cells *in vivo* (Compton et al., 2007) but, given the importance of this cell type in the stabilization and maintenance of the coronary vessels, we chose to directly test for any requirement of TGFβR3 in epicardial cell differentiation into smooth muscle. We have previously shown that TGFβ1 or TGFβ2 induces loss of epithelial character and smooth muscle differentiation in *Tgfbr3*$^{+/+}$ epicardial cells (Austin et al., 2008). Here, immunostaining revealed that both *Tgfbr3*$^{+/+}$ and *Tgfbr3*$^{-/-}$ cells have abundant expression of the tight junction protein zonula occludens-1 (ZO-1) at the cell borders (Fig. 3A). This pattern of ZO-1 expression is characteristic of epithelial cells (Lee et al., 2009b). In both *Tgfbr3*$^{+/+}$ and *Tgfbr3*$^{-/-}$ cells, 250 pM TGFβ1 or TGFβ2 caused the loss of cell border localization of ZO-1 indicative of the loss of epithelial character. These data are consistent with the analysis of *Tgfbr3*$^{-/-}$ embryos which show that epicardial cells can undergo EMT evident by the appearance of epicardially derived cells in the subepicardial space.

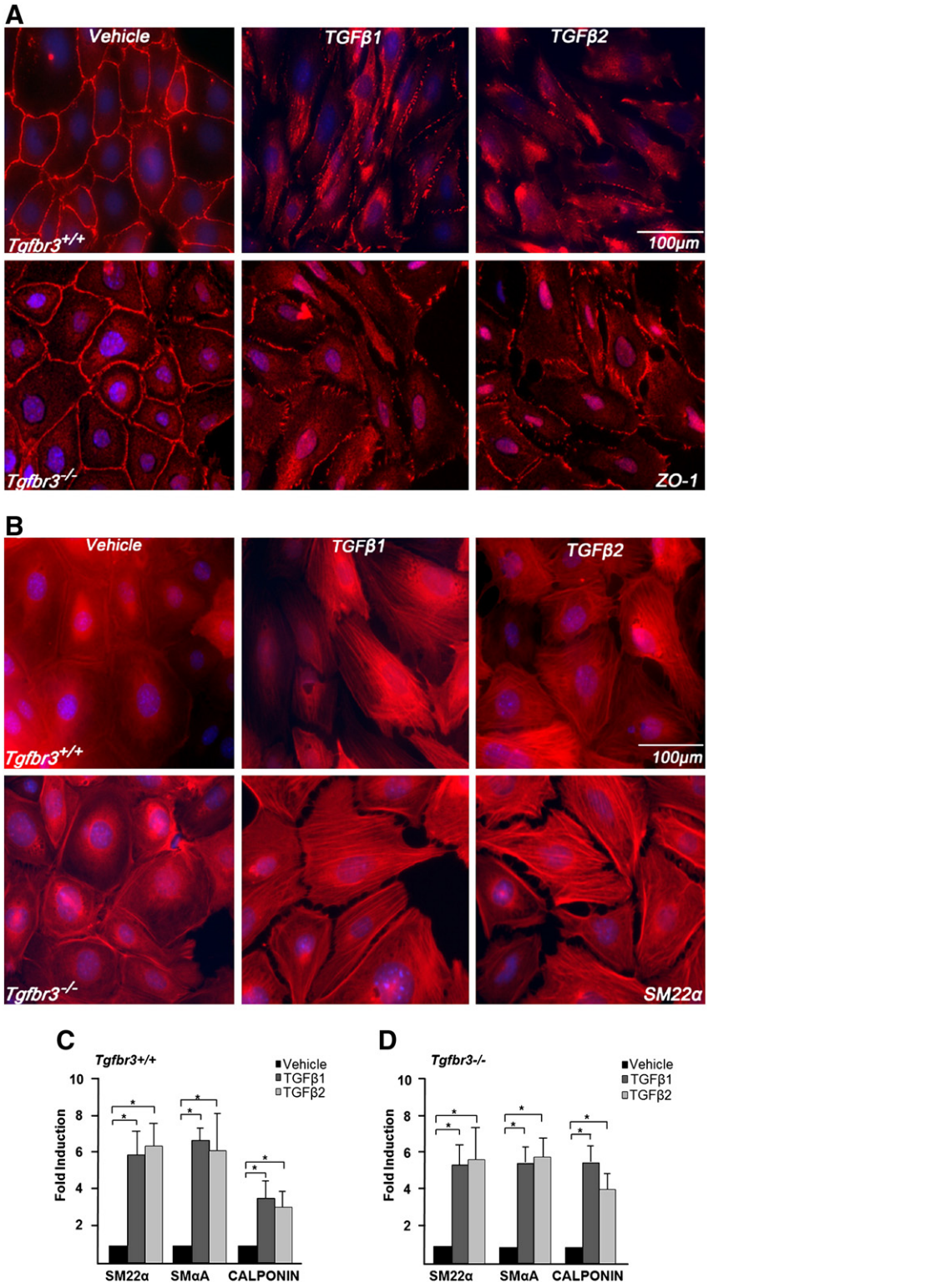


**Fig. 3.** Cultured *Tgfbr3*$^{-/-}$ epicardial cells can undergo EMT and smooth muscle differentiation. *Tgfbr3*$^{+/+}$ and *Tgfbr3*$^{-/-}$ cells were incubated with vehicle, 250 pM TGFβ1 or TGFβ2 for 72 h. (A) Immunohistochemistry: *Tgfbr3*$^{+/+}$ (top) and *Tgfbr3*$^{-/-}$ (bottom) cells incubated with vehicle localize the epithelial marker, ZO-1 to cell margins. TGFβ1 or TGFβ2 induces loss of cell–cell contact and loss of ZO-1 from cell margins. (B) *Tgfbr3*$^{+/+}$ (top) and *Tgfbr3*$^{-/-}$ (bottom) cells incubated with vehicle do not show SM22α in stress fibers. TGFβ1 or TGFβ2 induces SM22α expression in stress fibers in both genotypes. (C and D) Induction of the smooth muscle markers, SM22α, SMαA, and Calponin was evaluated using qRT-PCR analysis ($n=3$; $^{*}p<0.05$).

Loss of epithelial character was accompanied by the appearance of the smooth muscle marker SM22α in stress fibers (Fig. 3B). Smooth muscle marker expression was confirmed by qRT-PCR, and both TGFβ1 and TGFβ2 significantly induced the expression of SM22α, SMα-actin (SMαA), and calponin in *Tgfbr3*$^{-/-}$ cells (Figs. 3C and D). Together, these data demonstrate that *Tgfbr3* is not required for the loss of epithelial character or smooth muscle differentiation in epicardial cells and supports the conclusion that loss of the ability of epicardial cells to differentiate into smooth muscle is not a component of the phenotype of the *Tgfbr3*$^{-/-}$ mouse.

*Loss of TGFβR3 results in decreased responsiveness to not only TGFβ1 and TGFβ2 but to other key regulators of cell invasion*

Since the loss of *Tgfbr3* results in decreased cell invasion due to decreased TGFβ responsiveness, and several other growth factors have been shown to mediate epicardial EMT and invasion (Craig et al., 2010b; Mellgren et al., 2008; Morabito et al., 2001; Tomanek et al., 2001, 2002), we next asked if loss of *Tgfbr3* altered responsiveness to other key regulators of cell invasion. High molecular weight hyaluronic acid (HMW-HA), a major component of the ECM in the developing heart (Camenisch et al., 2000), has recently been implicated in mediating epicardial EMT and invasion (Craig et al., 2010b). Furthermore, TGFβ2 has been reported to regulate HAS-2 expression, the gene responsible for hyaluronic acid synthesis (Craig et al., 2010a). Given the decreased responsiveness to TGFβ2-induced invasion observed in $Tgfbr3^{-/-}$ cells *in vitro* and the role of HMW-HA in regulating epicardial cell behavior, we assessed the ability of $Tgfbr3^{+/+}$ and $Tgfbr3^{-/-}$ cells to invade collagen gels in response to HMW-HA. $Tgfbr3^{+/+}$ and $Tgfbr3^{-/-}$ cells were incubated with 0, 50, 75, 150 or 300 μg/ml HMW-HA, and cellular invasion analyzed. $Tgfbr3^{+/+}$ cells show a concentration dependent increase in invasion with HMW-HA, however, $Tgfbr3^{-/-}$ cells do not (Fig. 4A). To determine whether the loss of responsiveness to HMW-HA correlated with loss of HA receptor expression, we detected levels of the HA receptors, LYVE1 and CD44, using qRT-PCR and Western blot analysis. Protein and mRNA levels of both receptors are not significantly different between genotypes; hence decreased responsiveness to HMW-HA does not correlate with loss of HA receptor expression (Fig. 4B). Additional factors that mediate epicardial EMT and invasion include FGF2, PDGFAA, PDGFBB, EGF, and VEGF (Mellgren et al., 2008; Morabito et al., 2001; Tomanek et al., 2001, 2002). Therefore, to determine whether there is a global defect in the ability of $Tgfbr3^{-/-}$ cells to execute invasive cell motility, we assessed whether responsiveness to any of these factors was altered in $Tgfbr3^{-/-}$ cells. Response to PDGFAA, PDGFBB, EGF, and VEGF is unaltered between genotypes, however $Tgfbr3^{-/-}$ littermates display a decreased ability to invade in response to FGF2 (1.5-fold relative to vehicle), a potent inducer of epicardial cell EMT and invasion *in vitro* (Morabito et al., 2001), when compared to $Tgfbr3^{+/+}$ controls (2.25-fold relative to vehicle) (Fig. 4C). Analysis of receptor expression using qRT-PCR revealed no difference in FGF receptor expression (Fig. 4D). Collectively, these data suggests that $Tgfbr3^{-/-}$ cells are competent to execute invasive cell motility and reveal that TGFβR3 plays a central role in regulating responsiveness not only to members of the TGFβ family but select mediators of epicardial cell function such as HMW-HA and FGF2.

*Non-canonical signaling through TGFβR3 interaction with GIPC is required for invasion*

The mechanisms by which TGFβR3 signals are largely unknown. The cytoplasmic domain of TGFβR3 is not required to present ligand to TGFβR1 and TGFβR2 to augment canonical signaling (Blobe et al., 2001b). Targeting TGFβR3 in mice (Compton et al., 2007) and cardiac cushion explants (Brown et al., 1999) suggests a unique and non-redundant role for TGFβR3 in addition to ligand presentation. To determine a potential role of the cytoplasmic domain of TGFβR3 in regulating proliferation and invasion, we expressed TGFβR3 mutants missing portions of the cytoplasmic domain (Fig. 5A). The cytoplasmic domain of TGFβR3 lacks enzymatic activity but the 3 C-terminal amino acids bind the scaffolding protein GIPC1 (Blobe et al., 2001a). We overexpressed in $Tgfbr3^{-/-}$ cells either full length TGFβR3 (FL), TGFβR3 lacking the entire cytoplasmic domain (CYTO) or TGFβR3 lacking only the 3 C-terminal amino acids (Δ3) (Supplementary Figs. 5A–D). Overexpression of TGFβR3 FL in $Tgfbr3^{-/-}$ cells rescued both proliferation (Supplementary Fig. 6A) and TGFβ, HMW-HA, and FGF-2

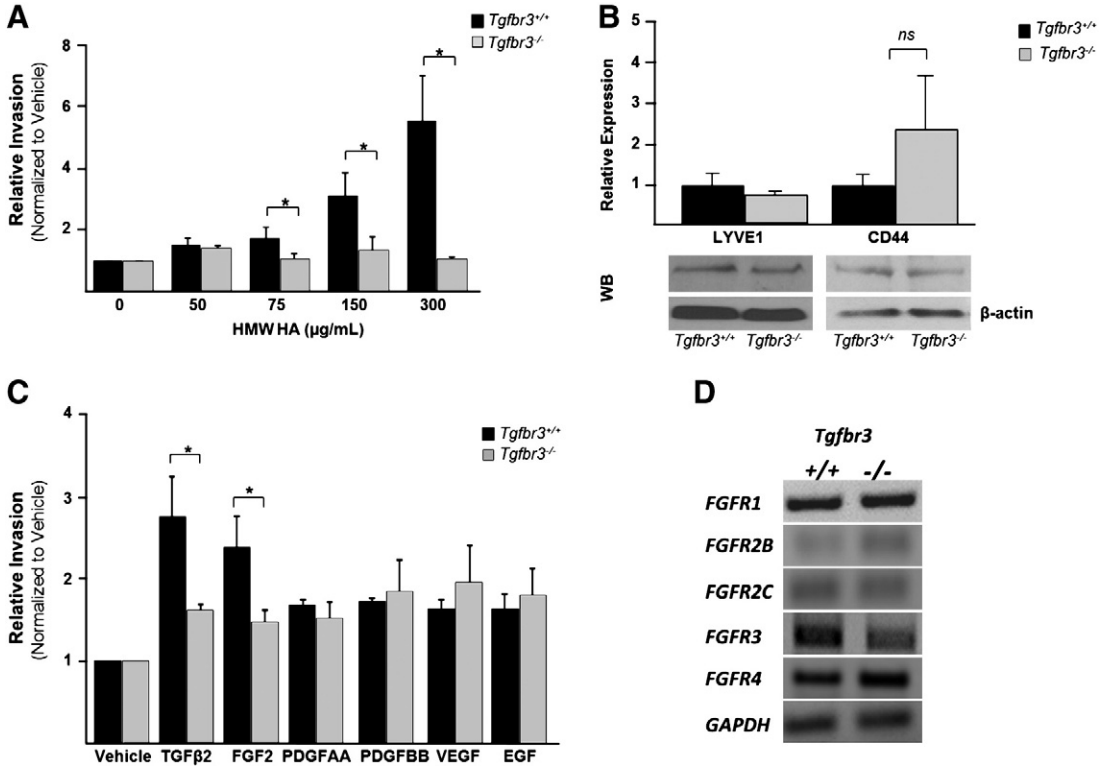


**Fig. 4.** Loss of *Tgfbr3* results in decreased response to HMW-HA and FGF-2. Invasion was analyzed as described in Fig. 2D for panels A and C. (A) Concentration response $Tgfbr3^{+/+}$ and $Tgfbr3^{-/-}$ littermate pair with HMW-HA. (B) Expression analysis using qRT-PCR (top) and western blot (bottom) comparing LYVE1 and CD44 levels in $Tgfbr3^{+/+}$ and $Tgfbr3^{-/-}$ littermate pair. (C) Incubation with vehicle, 250 pM TGFβ2, or 10 ng/ml of FGF2, PDGFAA, PDGFBB, VEGF or EGF. (Experiments repeated 3 times in replicates of 6, results for one littermate pair shown,* = $p<0.05$). (D) Expression analysis using qRT-PCR comparing FGFR levels in $Tgfbr3^{+/+}$ and $Tgfbr3^{-/-}$ littermate pair.

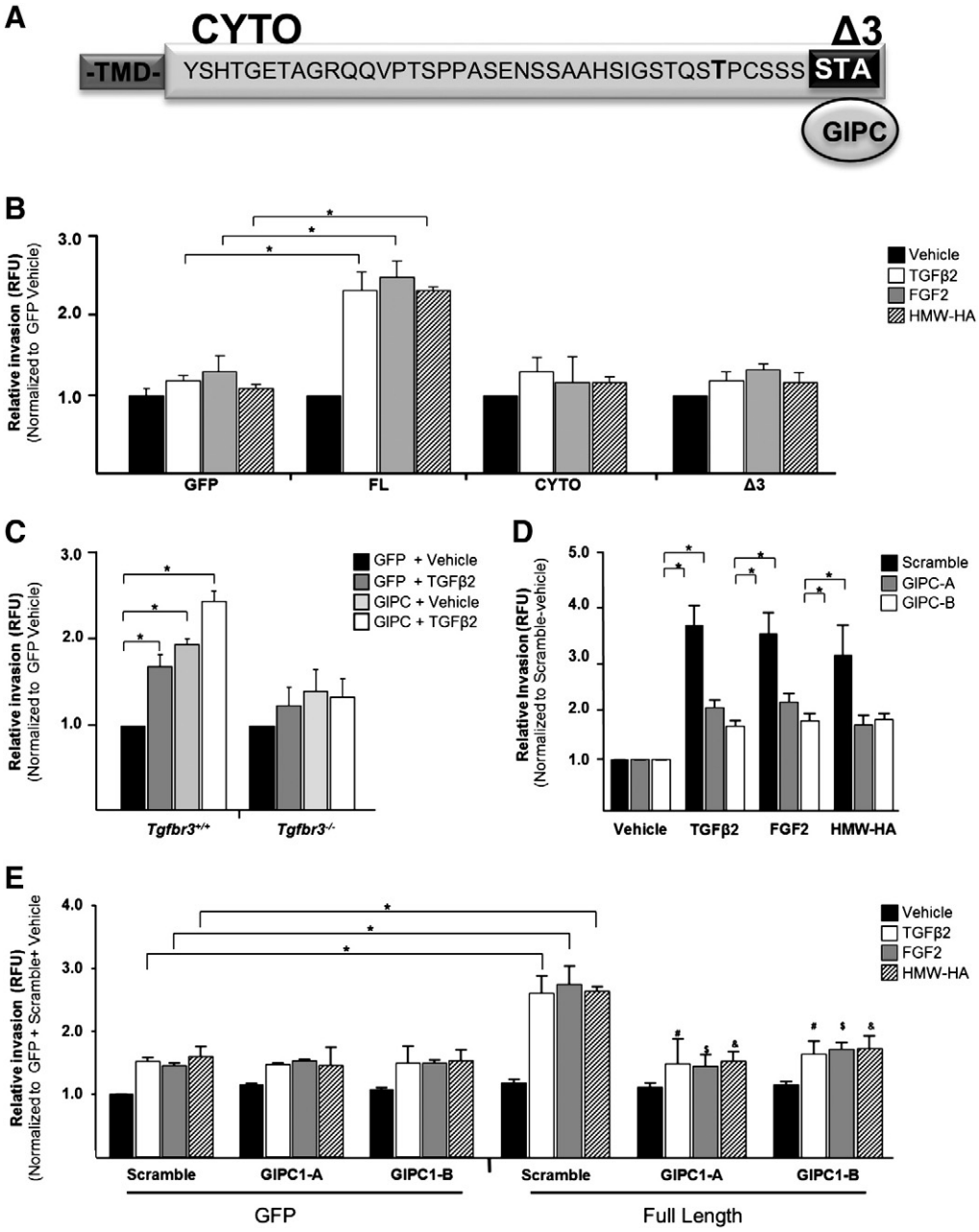


**Fig. 5.** The cytoplasmic domain of TGFβR3 and GIPC are required for invasion. Invasion was analyzed as described in Fig. 2D for all panels. (A) TGFβR3 contains a 43 amino acid cytoplasmic domain whose C-terminal 3 amino acids, STA, bind GIPC. (B) *Tgfbr3*$^{-/-}$ epicardial cells infected with adenovirus co-expressing GFP and either FL, CYTO or Δ3 receptor and incubated with vehicle, 250 pM TGFβ2, 10 ng/ml FGF-2 or 300 μg/ml HMW-HA. (C) *Tgfbr3*$^{+/+}$ or *Tgfbr3*$^{-/-}$ cells infected with adenovirus co-expressing GFP and GIPC1. (D) *Tgfbr3*$^{+/+}$ cells transfected with siRNA to GIPC1 and incubated with vehicle, 250 pM TGFβ2, 10 ng/ml FGF-2 or 300 μg/ml HMW-HA. (n = 3, replicates of 6,* = $p<0.05$). (E) *Tgfbr3*$^{-/-}$ cells infected with adenovirus expressing GFP or FL receptor, transfected with siRNA to GIPC1, and incubated with vehicle, 250 pM TGFβ2, 10 ng/ml FGF-2, or 300 μg/ml HMW-HA. (n = 3, replicates of 4). *[GFP + scramble + ligand] *vs.* [FL + scramble + ligand]; #[FL + scramble + TGFβ2] *vs.* [FL + GIPCsiRNA + TGFβ2]; $[FL + scramble + FGF2] *vs.* [FL + GIPCsiRNA + FGF2]; and&[FL + scramble + HMW-HA] *vs.* [FL + GIPCsiRNA + HMW-HA]; $p<0.05$.

mediated cellular invasion relative to vehicle incubated, GFP expressing cells (Fig. 5B). In contrast, overexpression of either TGFβR3 CYTO or Δ3 did not rescue proliferation (Supplementary Fig. 6A) or invasion in *Tgfbr3*$^{-/-}$ cells (Fig. 5B). These data demonstrate that the cytoplasmic domain, and specifically the 3 C-terminal amino acids, are required for the regulation of TGFβR3-mediated proliferation and invasion by epicardial cells.

The interaction between TGFβR3 and GIPC1, through the 3 C-terminal amino acids, has been reported to regulate cellular invasion in breast cancer cell lines (Lee et al., 2009a). Therefore, we assessed the role of GIPC in proliferation and invasion by overexpressing GIPC in *Tgfbr3*$^{+/+}$ and *Tgfbr3*$^{-/-}$ cells. Three isoforms of GIPC exist and we found GIPC1 is the predominant form in epicardial cells. Overexpression of GIPC1 had no effect on proliferation rate irrespective of genotype (Supplementary Fig. 6B). Overexpression of GIPC1 enhanced cellular invasion by *Tgfbr3*$^{+/+}$ cells but did not rescue deficient invasive cell motility by *Tg*fbr3$^{-/-}$ epicardial cells (Fig. 5C). Knockdown of GIPC1 with either one of two specific siRNA constructs in *Tgfbr3*$^{+/+}$ epicardial cells reduced TGFβ2, HMW-HA, and FGF-2-induced invasion to levels comparable to those observed in *Tgfbr3*$^{-/-}$ cells (Fig. 5D) while having no effect on cellular proliferation rates (Supplementary Figs. 6C and D). To directly establish that TGFβR3-mediated invasion in response to TGFβ2, FGF-2, and HMW-HA requires GIPC, we overexpressed TGFβR3-FL in

*Tgfbr3* $^{-/-}$ cells, knocked down GIPC1, and analyzed TGFβ2, FGF-2, and HMW-HA mediated invasion (Fig. 5E). The addition of GIPC1 siRNA to cells overexpressing TGFβR3-FL significantly inhibited the ability of TGFβR3-FL to mediate TGFβ2, FGF-2 or HMW-HA-induced invasion. These data support the requirement of GIPC for TGFβR3-mediated invasion in response to TGFβ2, HMW-HA, and FGF-2.

## Discussion

The loss of *Tgfbr3* in mice results in failed coronary vessel development (Compton et al., 2007) but the mechanisms by which TGFβR3 signals and regulates this process are largely unknown. Here we show that the loss of TGFβR3 is associated with decreased proliferation and invasion in both epicardial cells and the epicardium of intact embryos. Surprisingly, the decreased invasion of epicardial cells is seen in response to FGF2 and HMW-HA, known regulators of epicardial cell behavior and coronary vessel development (Craig et al., 2010b; Pennisi and Mikawa, 2009) in addition to TGFβ1 and TGFβ2. The responsiveness to these ligands in *Tgfbr3* $^{-/-}$ cells was found to be dependent on the 3 terminal amino acids of the cytoplasmic domain of TGFβR3 and interaction with GIPC indicating that TGFβR3 is signaling via a mechanism distinct from ligand presentation and activation of canonical TGFβ signaling. Based on our observations we propose that failed coronary vessel development in *Tgfbr3* $^{-/-}$ mice is due to decreased delivery of epicardially derived cells that are required to participate in coronary vessel development. We suggest that altered behavior in *Tgfbr3* $^{-/-}$ cells *in vivo* is at least partially due to the loss of signaling from FGF2 and HMW-HA as well as TGFβ. Since TGFβR3 signaling requires a specific cytoplasmic domain and the interacting protein GIPC to support epicardial cell invasion and responsiveness to TGFβ, FGF2, and HMW-HA, we propose that failed interaction between TGFβR3 and GIPC in the *Tgfbr3* $^{-/-}$ embryo is responsible for failed coronary vessel development (Fig. 6).

Our results showing that decreased proliferation and invasion are associated with failed coronary vessel development suggest that the time window during which cells must be delivered to the heart to participate in coronary vessel development is relatively narrow. A decrease in the number of cells available to participate in vessel formation may be tolerated in other vascular beds, but the dependence of embryo viability on coronary vessel formation by E15.0 does not allow sufficient time for the continued production and delivery of lower numbers of cells to rescue coronary vessel development. This is supported by several other gene knockouts that affect coronary vessel development that have reported altered proliferation, apoptosis, or invasion in the epicardium, epicardial-derived cells, or myocardium (Lavine et al., 2006; Li et al., 2002;

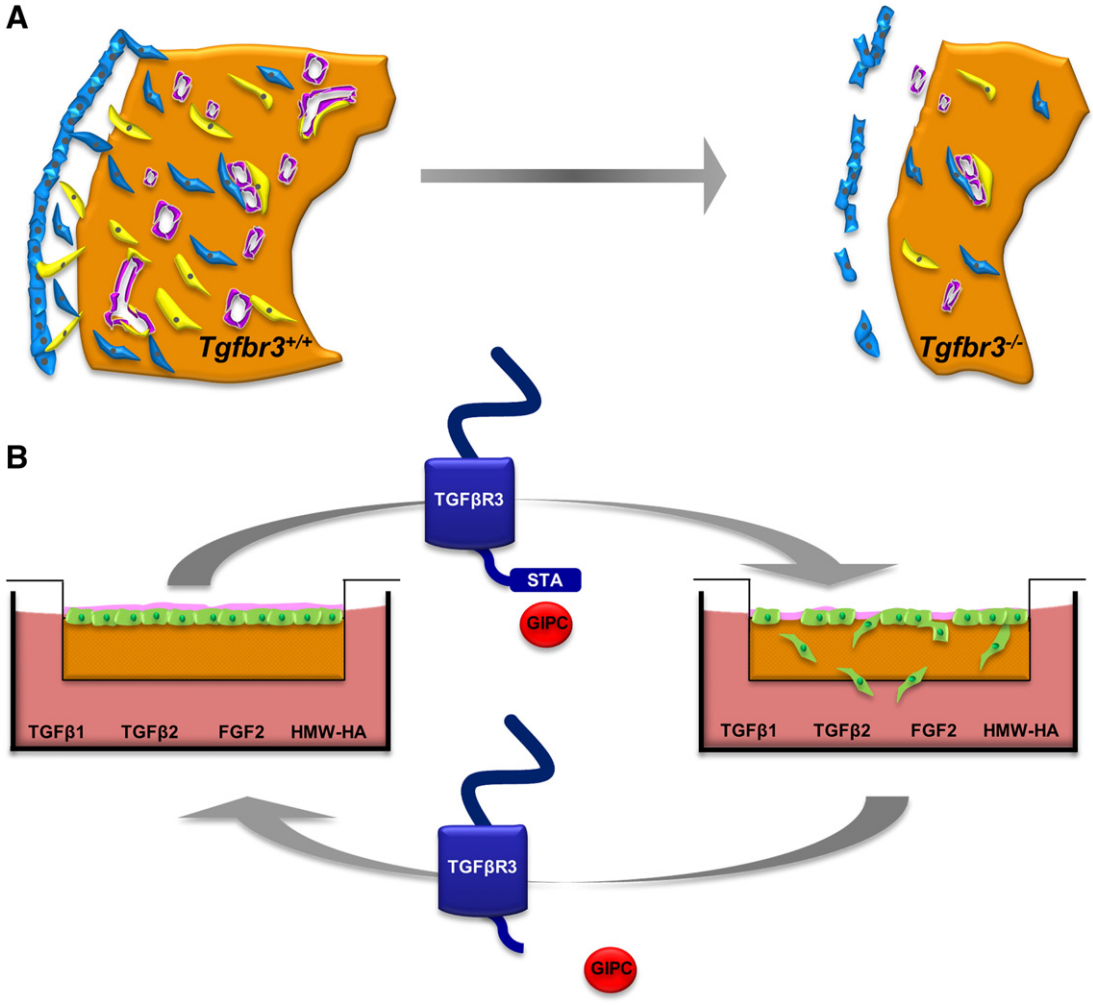


**Fig. 6.** Model of TGFβR3 regulation of epicardial cell behavior. (A) In *Tgfbr3* $^{+/+}$ hearts (left), the epicardium forms a continuous epicardial layer that is tightly opposed to the myocardium. Epicardial-derived cells (EPDCs) undergo EMT and invade the subepicardial space. Some of these cells invade the myocardium and become smooth muscle cells (yellow) and cardiac fibroblasts (blue) while endothelial cells (purple) are contributed by the sinus venosus. In *Tgfbr3* $^{-/-}$ hearts (right), decreased proliferation of epicardial cells and an impaired ability of these cells to invade results in fewer cells to participate in vessel development. (B) *In vitro*, the invasion deficit in *Tgfbr3* $^{-/-}$ cells seen in response TGFβ1, TGFβ2 FGF2, and HMW-HA can be rescued by TGFβR3-FL which allows interaction with GIPC. Expression of TGFβR3-Δ3 which lacks GIPC binding site, or targeting of GIPC, does not rescue invasion. These data suggest that TGFβR3 and GIPC interaction are also required for regulating epicardial cell behavior *in vivo*.

Mellgren et al., 2008; Rhee et al., 2009; Sridurongrit et al., 2008). Understanding the pathways that regulate epicardial cell proliferation and invasion during development has become increasingly important as a mounting amount of evidence demonstrate that pathways that regulate epicardial cell development are reinitiated during heart regeneration. Injury models in zebrafish uncovered a novel role for the epicardium in the regeneration of myocardium accompanied by the activation of developmental genes throughout the epicardium, epicardial cell EMT, and the appearance of new vessels (Lepilina et al., 2006). Mammals possess less regenerative capacity than zebrafish but analysis of the response of the epicardium to injury reveals striking similarities (Bock-Marquette et al., 2009; Cai et al., 2008; Christoffels et al., 2009; Rentschler and Epstein, 2011; Smart et al., 2007; Zhou et al., 2008). For example in mice, a novel population of cells derived from the epicardium have been found to increase after myocardial infarction or aortic banding consistent with a role in injury response (Russell et al., 2011). These data suggest that understanding the factors that regulate epicardial cell proliferation and invasion may provide the opportunity to target the epicardium to modulate the response to injury in adults.

We had the surprising result that loss of TGFβR3 also altered responsiveness to both HMW-HA and FGF2 despite unchanged levels of their respective receptors. This result was specific to HMW-HA and FGF2 since epicardial cell invasion in response to PDGFAA, PDGFBB, VEGF, and EGF is unaffected by the loss of TGFβR3. Both HMW-HA and FGF2 are important regulators of epicardial cell invasion (Craig et al., 2010b; Morabito et al., 2001). The loss of responsiveness of epicardial cells to FGF2 and HMW-HA, in addition to TGFβ1 and TGFβ2, may explain how the loss of a single gene, which disrupts several potential signaling pathways, so dramatically alters the morphology of the epicardium and myocardium in *Tgfbr3*$^{-/-}$ embryos. Altered myocardial morphology and decreased myocardial proliferation is noted in a number of mouse models where gene deletion alters the epicardium (Kwee et al., 1995; Mahtab et al., 2008; Sridurongrit et al., 2008) and likely reflects the well documented requirement of intact epicardial–myocardial interaction (Crispino et al., 2001; Kwee et al., 1995; Lavine et al., 2005; Merki et al., 2005; Olivey and Svensson, 2010; Tevosian et al., 2000; Yang et al., 1995) to support myocardial thickening (Weeke-Klimp et al., 2010; Wu et al., 1999). Decreased myocardial proliferation has also been reported in *Tgfbr3*$^{-/-}$ embryos (Stenvers et al., 2003). Our results suggest a dysregulation of the ability of *Tgfbr3*$^{-/-}$ cells to respond to several known regulators of epicardial and coronary vessel development (Craig et al., 2010b; Pennisi and Mikawa, 2009) and establishes TGFβR3 as a regulator of multiple signals that direct epicardial cell behavior.

Examination of the ability to rescue the deficits seen in *Tgfbr3*$^{-/-}$ cells by TGFβR3 mutants indicates a role for noncanonical TGFβ signaling in the regulation of epicardial cell proliferation and invasion. The expression of TGFβR3-CYTO or TGFβR3-Δ3 is unable to rescue demonstrating the requirement of the cytoplasmic domain, and specifically the 3 C-terminal amino acids, for signaling. Importantly, the cytoplasmic domain of TGFβR3 is not required for ligand presentation and signaling via the canonical TGFβ pathway (Blobe et al., 2001a). How can the rescue of FGF2 and HMW-HA be explained? These ligands could bind TGFβR3 and initiate signaling or these ligands could activate signaling through their respective receptors that share a common downstream mediator that is lost in *Tgfbr3*$^{-/-}$ cells. In support of directly signaling through TGFβR3, it has been reported that FGF2 can bind to TGFβR3 (Andres et al., 1992) and more recent data in valvular interstitial cells demonstrates a functional link between FGF2 binding and TGFβR3 activation (Han and Gotlieb, 2011). In contrast, HMW-HA has not been reported to bind TGFβR3 consistent with the idea that TGFβ, FGF2, and HMW-HA may share a common downstream mediator that is dysregulated in the absence of TGFβR3.

The inability of TGFβR3-Δ3 to rescue identified a potential mediator of this noncanonical pathway downstream of TGFβR3. The scaffolding protein GIPC1 requires these same 3 C-terminal amino acids to bind TGFβR3 (Blobe et al., 2001a). Interaction between TGFβR3 and GIPC1 in cancer cell lines regulates cell migration and invasion (Lee et al., 2009a), while the targeted deletion of GIPC1, or synectin, in mice has been shown to attenuate the growth and branching of coronary arterioles (Dedkov et al., 2007). In endothelial cells, the interaction of GIPC1 with syndecan-4, a co-receptor for FGF2, (Tkachenko et al., 2006) or endoglin, a coreceptor for TGFβ, (Lee et al., 2008) has been shown to regulate migration. Consistent with the known role of the 3 C terminal amino acids of TGFβR3 in GIPC binding (Blobe et al., 2001a), siRNA directed against GIPC1 decreased invasion of *Tgfbr3*$^{+/+}$ cells in response to TGFβ2, FGF2, or HMW-HA, phenocopying loss of *Tgfbr3*. Further, siRNA directed against GIPC1 prevented rescue of invasion by TGFβR3-FL in *Tgfbr3*$^{-/-}$ cells. Taken together, our data in epicardial cells are most consistent with the interaction between the 3 C-terminal amino acids of the cytoplasmic domain of TGFβR3 and GIPC being required for the regulation of invasion. We conclude that TGFβR3 signaling via a noncanonical signaling pathway that includes interaction with GIPC1 plays a key role in epicardial cell function during coronary vessel development and may provide a potential novel target for therapies directed at the epicardium and epicardial derivatives.

In summary, *Tgfbr3*$^{-/-}$ mice have failed coronary vessel development accompanied by hyperplasia of the subepicardial layer (Compton et al., 2007) indicating that epicardial cells can undergo EMT and enter the subepicardial matrix. Based on our observations we propose that failed coronary vessel development in *Tgfbr3*$^{-/-}$ mice is at least partly due to decreased epicardial cell proliferation and mesenchymal cell invasion which limits the number of cells available to participate in coronary vessel development (Fig. 6). We had the unexpected result that *Tgfbr3*$^{-/-}$ epicardial cells have decreased responsiveness to FGF2 and HA in addition to TGFβ and we suggest that altered epicardial cell behavior in *Tgfbr3*$^{-/-}$ cells is at least partially due to the loss of signaling from these cues. Surprisingly, we found that TGFβR3 signaling requires a specific cytoplasmic domain and the interacting protein GIPC to support epicardial cells invasion and responsiveness to TGFβ, FGF2, and HMW-HA. We propose that this failed interaction in the *Tgfbr3*$^{-/-}$ embryo is responsible for failed coronary vessel development.

Supplementary materials related to this article can be found online at doi:10.1016/j.ydbio.2011.08.008.

## Sources of funding

This work was supported by NIH Grant HL085708 (JVB, JDL, JHS), GM007628 (NSS), HL087136 (AC) and American Heart Association AHA0655129 (JVB, CRH).

## Acknowledgments

We acknowledge Mark Frey, Ph.D. for his help with wound healing assay and Edina Kosa, M. Sc., for technical assistance in the 2D motility studies. We thank Florent Elefteriou, Ph.D., Vivian Siegel, Ph.D., Patricia A. Labosky, Ph.D., and Antonis K, Hatzopoulos, Ph.D., for critical feedback of this manuscript. J.V.B acknowledges the support of the Vanderbilt Ingram Cancer Center.

## References

Andres, J.L., DeFalcis, D., Noda, M., Massague, J., 1992. Binding of two growth factor families to separate domains of the proteoglycan betaglycan. J. Biol. Chem. 267, 5927–5930.

Austin, A.F., Compton, L.A., Love, J.D., Brown, C.B., Barnett, J.V., 2008. Primary and immortalized mouse epicardial cells undergo differentiation in response to TGFbeta. Dev. Dyn. 237, 366–376.

Blobe, G.C., Liu, X., Fang, S.J., How, T., Lodish, H.F., 2001a. A novel mechanism for regulating transforming growth factor beta (TGF-beta) signaling. Functional modulation of type III TGF-beta receptor expression through interaction with the PDZ domain protein, GIPC. J. Biol. Chem. 276, 39608–39617.

Blobe, G.C., Schiemann, W.P., Pepin, M.C., Beauchemin, M., Moustakas, A., Lodish, H.F., O'Connor-McCourt, M.D., 2001b. Functional roles for the cytoplasmic domain of the

type III transforming growth factor beta receptor in regulating transforming growth factor beta signaling. J. Biol. Chem. 276, 24627–24637.
Bock-Marquette, I., Shrivastava, S., Pipes, G.C., Thatcher, J.E., Blystone, A., Shelton, J.M., Galindo, C.L., Melegh, B., Srivastava, D., Olson, E.N., DiMaio, J.M., 2009. Thymosin beta4 mediated PKC activation is essential to initiate the embryonic coronary developmental program and epicardial progenitor cell activation in adult mice in vivo. J. Mol. Cell. Cardiol. 46, 728–738.
Brown, C.B., Boyer, A.S., Runyan, R.B., Barnett, J.V., 1999. Requirement of type III TGF-beta receptor for endocardial cell transformation in the heart. Science 283, 2080–2082.
Cai, C.L., Martin, J.C., Sun, Y., Cui, L., Wang, L., Ouyang, K., Yang, L., Bu, L., Liang, X., Zhang, X., Stallcup, W.B., Denton, C.P., McCulloch, A., Chen, J., Evans, S.M., 2008. A myocardial lineage derives from Tbx18 epicardial cells. Nature 454, 104–108.
Camenisch, T.D., Spicer, A.P., Brehm-Gibson, T., Biesterfeldt, J., Augustine, M.L., Calabro Jr., A., Kubalak, S., Klewer, S.E., McDonald, J.A., 2000. Disruption of hyaluronan synthase-2 abrogates normal cardiac morphogenesis and hyaluronan-mediated transformation of epithelium to mesenchyme. J. Clin. Invest. 106, 349–360.
Chen, W., Kirkbride, K.C., How, T., Nelson, C.D., Mo, J., Frederick, J.P., Wang, X.F., Lefkowitz, R.J., Blobe, G.C., 2003. Beta-arrestin 2 mediates endocytosis of type III TGF-beta receptor and down-regulation of its signaling. Science 301, 1394–1397.
Christoffels, V.M., Grieskamp, T., Norden, J., Mommersteeg, M.T., Rudat, C., Kispert, A., 2009. Tbx18 and the fate of epicardial progenitors. Nature 458, E8–E9 discussion E9-10.
Compton, L.A., Potash, D.A., Brown, C.B., Barnett, J.V., 2007. Coronary vessel development is dependent on the type III transforming growth factor beta receptor. Circ. Res. 101, 784–791.
Craig, E.A., Parker, P., Austin, A.F., Barnett, J.V., Camenisch, T.D., 2010a. Involvement of the MEKK1 signaling pathway in the regulation of epicardial cell behavior by hyaluronan. Cell. Signal. 22, 968–976.
Craig, E.A., Austin, A.F., Vaillancourt, R.R., Barnett, J.V., Camenisch, T.D., 2010b. TGFbeta2-mediated production of hyaluronan is important for the induction of epicardial cell differentiation and invasion. Exp. Cell Res. 968–976.
Crispino, J.D., Lodish, M.B., Thurberg, B.L., Litovsky, S.H., Collins, T., Molkentin, J.D., Orkin, S.H., 2001. Proper coronary vascular development and heart morphogenesis depend on interaction of GATA-4 with FOG cofactors. Genes Dev. 15, 839–844.
Dedkov, E.I., Thomas, M.T., Sonka, M., Yang, F., Chittenden, T.W., Rhodes, J.M., Simons, M., Ritman, E.L., Tomanek, R.J., 2007. Synectin/syndecan-4 regulate coronary arteriolar growth during development. Dev. Dyn. 236, 2004–2010.
Derynck, R., Zhang, Y.E., 2003. Smad-dependent and Smad-independent pathways in TGF-beta family signalling. Nature 425, 577–584.
Gittenberger-de Groot, A.C., Vrancken Peeters, M.P., Mentink, M.M., Gourdie, R.G., Poelmann, R.E., 1998. Epicardium-derived cells contribute a novel population to the myocardial wall and the atrioventricular cushions. Circ. Res. 82, 1043–1052.
Grieskamp, T., Rudat, C., Ludtke, T.H., Norden, J., Kispert, A., 2011. Notch signaling regulates smooth muscle differentiation of epicardium-derived cells. Circ. Res. 108, 813–823.
Han, L., Gotlieb, A.I., 2011. Fibroblast growth factor-2 promotes in vitro mitral valve interstitial cell repair through transforming growth factor-beta/Smad signaling. Am. J. Pathol. 178, 119–127.
He, T.-C., Zhou, S., da Costa, L.T., Yu, J., Kinzler, K.W., Vogelstein, B., 1998. A simplified system for generating recombinant adenoviruses. Proc. Natl. Acad. Sci. U.S.A. 95, 2509–2514.
Kirkbride, K.C., Townsend, T.A., Bruinsma, M.W., Barnett, J.V., Blobe, G.C., 2008. Bone morphogenetic proteins signal through the transforming growth factor-beta type III receptor. J. Biol. Chem. M704883200.
Kwee, L., Baldwin, H.S., Shen, H.M., Stewart, C.L., Buck, C., Buck, C.A., Labow, M.A., 1995. Defective development of the embryonic and extraembryonic circulatory systems in vascular cell adhesion molecule (VCAM-1) deficient mice. Development 121, 489–503.
Lavine, K.J., Yu, K., White, A.C., Zhang, X., Smith, C., Partanen, J., Ornitz, D.M., 2005. Endocardial and epicardial derived FGF signals regulate myocardial proliferation and differentiation in vivo. Dev. Cell 8, 85–95.
Lavine, K.J., White, A.C., Park, C., Smith, C.S., Choi, K., Long, F., Hui, C.C., Ornitz, D.M., 2006. Fibroblast growth factor signals regulate a wave of Hedgehog activation that is essential for coronary vascular development. Genes Dev. 20, 1651–1666.
Lavine, K.J., Long, F., Choi, K., Smith, C., Ornitz, D.M., 2008. Hedgehog signaling to distinct cell types differentially regulates coronary artery and vein development. Development 135, 3161–3171.
Lee, N.Y., Ray, B., How, T., Blobe, G.C., 2008. Endoglin promotes transforming growth factor beta-mediated Smad 1/5/8 signaling and inhibits endothelial cell migration through its association with GIPC. J. Biol. Chem. 283, 32527–32533.
Lee, J.D., Hempel, N., Lee, N.Y., Blobe, G.C., 2009a. The type III TGF-{beta} receptor suppresses breast cancer progression through GIPC-mediated inhibition of TGF-{beta} signaling. Carcinogenesis 31, 175–183.
Lee, N.Y., Kirkbride, K.C., Sheu, R.D., Blobe, G.C., 2009b. The transforming growth factor-beta type III receptor mediates distinct subcellular trafficking and downstream signaling of activin-like kinase (ALK)3 and ALK6 receptors. Mol. Biol. Cell 20, 4362–4370.
Lepilina, A., Coon, A.N., Kikuchi, K., Holdway, J.E., Roberts, R.W., Burns, C.G., Poss, K.D., 2006. A dynamic epicardial injury response supports progenitor cell activity during zebrafish heart regeneration. Cell 127, 607–619.
Li, W.E., Waldo, K., Linask, K.L., Chen, T., Wessels, A., Parmacek, M.S., Kirby, M.L., Lo, C.W., 2002. An essential role for connexin43 gap junctions in mouse coronary artery development. Development 129, 2031–2042.
Lie-Venema, H., van den Akker, N.M., Bax, N.A., Winter, E.M., Maas, S., Kekarainen, T., Hoeben, R.C., deRuiter, M.C., Poelmann, R.E., Gittenberger-de Groot, A.C., 2007. Origin, fate, and function of epicardium-derived cells (EPDCs) in normal and abnormal cardiac development. ScientificWorldJournal 7, 1777–1798.
Lie-Venema, H., Eralp, I., Markwald, R.R., van den Akker, N.M.S., Wijffels, M.C.E.F., Kolditz, D.P., van der Laarse, A., Schalij, M.J., Poelmann, R.E., Bogers, A.J.J.C., Gittenberger-de Groot, A.C., 2008. Periostin expression by epicardium-derived cells is involved in the development of the atrioventricular valves and fibrous heart skeleton. Differentiation 76, 809–819.
Lopez-Casillas, F., Cheifetz, S., Doody, J., Andres, J.L., Lane, W.S., Massague, J., 1991. Structure and expression of the membrane proteoglycan betaglycan, a component of the TGF-beta receptor system. Cell 67, 785–795.
Lopez-Casillas, F., Wrana, J.L., Massague, J., 1993. Betaglycan presents ligand to the TGF beta signaling receptor. Cell 73, 1435–1444.
Mahtab, E.A., Wijffels, M.C., Van Den Akker, N.M., Hahurij, N.D., Lie-Venema, H., Wisse, L.J., Deruiter, M.C., Uhrin, P., Zaujec, J., Binder, B.R., Schalij, M.J., Poelmann, R.E., Gittenberger-De Groot, A.C., 2008. Cardiac malformations and myocardial abnormalities in podoplanin knockout mouse embryos: correlation with abnormal epicardial development. Dev. Dyn. 237, 847–857.
Manner, J., 1993. Experimental study on the formation of the epicardium in chick embryos. Anat. Embryol. (Berl.) 187, 281–289.
Mellgren, A.M., Smith, C.L., Olsen, G.S., Eskiocak, B., Zhou, B., Kazi, M.N., Ruiz, F.R., Pu, W.T., Tallquist, M.D., 2008. Platelet-derived growth factor receptor beta signaling is required for efficient epicardial cell migration and development of two distinct coronary vascular smooth muscle cell populations. Circ. Res. 103, 1393–1401.
Merki, E., Zamora, M., Raya, A., Kawakami, Y., Wang, J., Zhang, X., Burch, J., Kubalak, S.W., Kaliman, P., Belmonte, J.C., Chien, K.R., Ruiz-Lozano, P., 2005. Epicardial retinoid X receptor alpha is required for myocardial growth and coronary artery formation. Proc. Natl. Acad. Sci. U.S.A. 102, 18455–18460.
Mikawa, T., Fischman, D.A., 1992. Retroviral analysis of cardiac morphogenesis: discontinuous formation of coronary vessels. Proc. Natl. Acad. Sci. U.S.A. 89, 9504–9508.
Mikawa, T., Gourdie, R.G., 1996. Pericardial mesoderm generates a population of coronary smooth muscle cells migrating into the heart along with ingrowth of the epicardial organ. Dev. Biol. 174, 221–232.
Moore, A., McInnes, L., Kreidberg, J., Hastie, N., Schedl, A., 1999. YAC complementation shows a requirement for Wt1 in the development of epicardium, adrenal gland and throughout nephrogenesis. Development 126, 1845–1857.
Morabito, C.J., Dettman, R.W., Kattan, J., Collier, J.M., Bristow, J., 2001. Positive and negative regulation of epicardial–mesenchymal transformation during avian heart development. Dev. Biol. 234, 204–215.
Mythreye, K., Blobe, G.C., 2009. The type III TGF-beta receptor regulates epithelial and cancer cell migration through beta-arrestin2-mediated activation of Cdc42. Proc. Natl. Acad. Sci. U.S.A. 106, 8221–8226.
Olivey, H.E., Svensson, E.C., 2010. Epicardial–myocardial signaling directing coronary vasculogenesis. Circ. Res. 106, 818–832.
Olivey, H.E., Compton, L.A., Barnett, J.V., 2004. Coronary vessel development: the epicardium delivers. Trends Cardiovasc. Med. 14, 247–251.
Pennisi, D.J., Mikawa, T., 2009. FGFR-1 is required by epicardium-derived cells for myocardial invasion and correct coronary vascular lineage differentiation. Dev. Biol. 328, 148–159.
Perryn, E.D., Czirok, A., Little, C.D., 2008. Vascular sprout formation entails tissue deformations and VE-cadherin-dependent cell-autonomous motility. Dev. Biol. 313, 545–555.
Poelmann, R.E., Gittenberger-de Groot, A.C., Mentink, M.M., Bokenkamp, R., Hogers, B., 1993. Development of the cardiac coronary vascular endothelium, studied with antiendothelial antibodies, in chicken-quail chimeras. Circ. Res. 73, 559–568.
Quarto, N., Longaker, M.T., 2008. Differential expression of specific FGF ligands and receptor isoforms during osteogenic differentiation of mouse Adipose-derived Stem Cells (mASCs) recapitulates the in vivo osteogenic pattern. Gene 424, 130–140.
Red-Horse, K., Ueno, H., Weissman, I.L., Krasnow, M.A., 2010. Coronary arteries form by developmental reprogramming of venous cells. Nature 464, 549–553.
Rentschler, S., Epstein, J.A., 2011. Kicking the epicardium up a notch. Circ. Res. 108, 6–8.
Rhee, D.Y., Zhao, X.Q., Francis, R.J., Huang, G.Y., Mably, J.D., Lo, C.W., 2009. Connexin 43 regulates epicardial cell polarity and migration in coronary vascular development. Development 136, 3185–3193.
Runyan, R.B., Markwald, R.R., 1983. Invasion of mesenchyme into three-dimensional collagen gels: a regional and temporal analysis of interaction in embryonic heart tissue. Dev. Biol. 95, 108–114.
Rupp, P.A., Visconti, R.P., Czirok, A., Cheresh, D.A., Little, C.D., 2008. Matrix metalloproteinase 2-integrin alpha(v)beta3 binding is required for mesenchymal cell invasive activity but not epithelial locomotion: a computational time-lapse study. Mol. Biol. Cell 19, 5529–5540.
Russell, J.L., Goetsch, S.C., Gaiano, N.R., Hill, J.A., Olson, E.N., Schneider, J.W., 2011. A dynamic notch injury response activates epicardium and contributes to fibrosis repair. Circ. Res. 108, 51–59.
Smart, N., Risebro, C.A., Melville, A.A., Moses, K., Schwartz, R.J., Chien, K.R., Riley, P.R., 2007. Thymosin beta4 induces adult epicardial progenitor mobilization and neovascularization. Nature 445, 177–182.
Sridurongrit, S., Larsson, J., Schwartz, R., Ruiz-Lozano, P., Kaartinen, V., 2008. Signaling via the Tgf-beta type I receptor Alk5 in heart development. Dev. Biol. 322, 208–218.
Stenvers, K.L., Tursky, M.L., Harder, K.W., Kountouri, N., Amatayakul-Chantler, S., Grail, D., Small, C., Weinberg, R.A., Sizeland, A.M., Zhu, H.J., 2003. Heart and liver defects and reduced transforming growth factor beta2 sensitivity in transforming growth factor beta type III receptor-deficient embryos. Mol. Cell. Biol. 23, 4371–4385.
Tevosian, S.G., Deconinck, A.E., Tanaka, M., Schinke, M., Litovsky, S.H., Izumo, S., Fujiwara, Y., Orkin, S.H., 2000. FOG-2, a cofactor for GATA transcription factors, is essential for heart morphogenesis and development of coronary vessels from epicardium. Cell 101, 729–739.
Tkachenko, E., Elfenbein, A., Tirziu, D., Simons, M., 2006. Syndecan-4 clustering induces cell migration in a PDZ-dependent manner. Circ. Res. 98, 1398–1404.
Tomanek, R.J., 2005. Formation of the coronary vasculature during development. Angiogenesis 8, 273–284.

Tomanek, R.J., Zheng, W., Peters, K.G., Lin, P., Holifield, J.S., Suvarna, P.R., 2001. Multiple growth factors regulate coronary embryonic vasculogenesis. Dev. Dyn. 221, 265–273.
Tomanek, R.J., Holifield, J.S., Reiter, R.S., Sandra, A., Lin, J.J., 2002. Role of VEGF family members and receptors in coronary vessel formation. Dev. Dyn. 225, 233–240.
Tomanek, R.J., Ishii, Y., Holifield, J.S., Sjogren, C.L., Hansen, H.K., Mikawa, T., 2006. VEGF family members regulate myocardial tubulogenesis and coronary artery formation in the embryo. Circ. Res. 98, 947–953.
Viragh, S., Challice, C.E., 1981. The origin of the epicardium and the embryonic myocardial circulation in the mouse. Anat. Rec. 201, 157–168.
Wang, X.F., Lin, H.Y., Ng-Eaton, E., Downward, J., Lodish, H.F., Weinberg, R.A., 1991. Expression cloning and characterization of the TGF-beta type III receptor. Cell 67, 797–805.
Weeke-Klimp, A., Bax, N.A.M., Bellu, A.R., Winter, E.M., Vrolijk, J., Plantinga, J., Maas, S., Brinker, M., Mahtab, E.A.F., Gittenberger-de Groot, A.C., van Luyn, M.J.A., Harmsen, M.C., Lie-Venema, H., 2010. Epicardium-derived cells enhance proliferation, cellular maturation and alignment of cardiomyocytes. J. Mol. Cell. Cardiol. 49, 606–616.
Wiater, E., Harrison, C.A., Lewis, K.A., Gray, P.C., Vale, W.W., 2006. Identification of distinct inhibin and transforming growth factor beta-binding sites on betaglycan: functional separation of betaglycan co-receptor actions. J. Biol. Chem. 281, 17011–17022.
Wu, K., Gauthier, D., Levine, M.D., 1995. Live cell image segmentation. IEEE Trans. Biomed. Eng. 42, 1–12.
Wu, H., Lee, S.H., Gao, J., Liu, X., Iruela-Arispe, M.L., 1999. Inactivation of erythropoietin leads to defects in cardiac morphogenesis. Development 126, 3597–3605.
Xiong, J.W., 2008. Molecular and developmental biology of the hemangioblast. Dev. Dyn. 237, 1218–1231.
Yang, J.T., Rayburn, H., Hynes, R.O., 1995. Cell adhesion events mediated by alpha 4 integrins are essential in placental and cardiac development. Development 121, 549–560.
You, H.J., How, T., Blobe, G.C., 2009. The type III transforming growth factor-{beta} receptor negatively regulates nuclear factor-{kappa}B signaling through its interaction with {beta}-arrestin2. Carcinogenesis 30, 1281–1287.
Zamir, E.A., Czirok, A., Rongish, B.J., Little, C.D., 2005. A digital image-based method for computational tissue fate mapping during early avian morphogenesis. Ann. Biomed. Eng. 33, 854–865.
Zhou, B., Ma, Q., Rajagopal, S., Wu, S.M., Domian, I., Rivera-Feliciano, J., Jiang, D., von Gise, A., Ikeda, S., Chien, K.R., Pu, W.T., 2008. Epicardial progenitors contribute to the cardiomyocyte lineage in the developing heart. Nature 454, 109–113.